



PERGAMON

Available online at www.sciencedirect.com



ACTA
ASTRONAUTICA

Acta Astronautica III (III) III-III

www.elsevier.com/locate/actaastro

Design of Earth–Mars transfer trajectories using evolutionary-branching technique[☆]

Massimiliano Vasile^{a,*}, Leopold Summerer^a, Paolo De Pascale^b

^aESA-ESTEC, Advanced Concepts Team, Keplerlaan 1, 2200 AZ, Noordwijk ZH, The Netherlands

^bPolitecnico di Milano, via La Masa 34, 2158 Milano, Italy

Received 11 February 2004; received in revised form 6 August 2004; accepted 7 December 2004

Abstract

In this paper a novel global optimisation approach is used to search for potentially interesting solutions for a mission to Mars. The approach blends the characteristics of evolutionary algorithms with the systematic search, typical of branching techniques. Solutions for a roundtrip to Mars, either direct or via Venus, considering long and short stays on Mars or free return trajectories are considered, thus providing a comprehensive view of all the opportunities within a wide range of possible launch dates. Finally, electric propulsion options are investigated including the possibility of using Mars' Lagrangian points for a low cost capture. The proposed global search was effectively able to find globally minimal Δv solutions for Earth–Mars roundtrips giving the expected characterisation of the problem under study. Moreover, it will be shown how the method was able to automatically rediscover known solutions along with new ones of practical interest for future Mars exploration.

© 2005 Published by Elsevier Ltd.

1. Introduction

In recent years the space community has demonstrated a growing interest in global optimisation techniques as a viable tool for the design of space trajectories [1–5]. However, most of the global methods

used so far can be classified as stochastic or heuristic approaches and in particular the evolutionary strategy [6–8] class, which represents only a portion of all available global methods [9]. In many cases they have proven to explore efficiently the solution space providing even unexpected optimal solutions or a number of good initial guesses useful for a further optimisation with more accurate local optimisation techniques.

Other classes of global methods like deterministic ones, such as branching or branch and bounds approaches, have received less attention even though they have been demonstrated to be extremely effective in many other fields [9–12]. A hybridisation of both stochastic and deterministic approaches could be

[☆] Based on paper IAC-03-A.7.07 presented at the 54th International Astronautical Congress, 29 September–3 October 2003, Bremen, Germany.

* Corresponding author. Tel.: +39 02 2399 8370.

E-mail address: vasile@aero.polimi.it (M. Vasile).

¹ Presently working at the Aerospace Department of Politecnico di Milano.

beneficial in the improvement of the effectiveness of both at solving space-related problems.

In this paper an analysis of a variety of Earth–Mars transfer trajectories has been performed using an innovative global optimisation approach, which combines a stochastic and a deterministic method.

The basic idea of this novel approach is to use a limited set of potential solutions evolving for a small number of generations, according to some specific evolution strategies (the stochastic step), in subregions of the solution space defined by a branching procedure (the deterministic step). On the other hand, the branching rules, i.e. the rules used to partition the solutions space, are functions of the outcome from the evolution step. This technique has been used to conduct an extensive search for families of potentially interesting transfer trajectories from Earth to Mars, and return, in view of future exploration and colonisation missions envisaged by the Aurora programme [13]. Several types of trajectories have been modelled including: multiple impulsive transfers, low thrust propulsion trajectories and indirect transfers, exploiting gravity-assisted manoeuvres or 3rd body dynamics in order to reduce either the transfer time or propellant consumption.

After an introduction of the proposed global optimisation approach, the paper presents some interesting results obtained analysing possible viable Earth–Mars transfers for the Aurora programme. On the one hand, these results represent a proof of the effectiveness of the methodology, on the other hand, they are a set of potentially useful solutions for future Mars missions.

2. General problem formulation

Optimisation problems in trajectory design can be formulated, in their general form, as

$$\min f(\mathbf{y})$$

$$\mathbf{b}^l \leq \mathbf{C}(\mathbf{y}) \leq \mathbf{b}^u$$

$$\text{with } \mathbf{y} \in D, \quad (1)$$

where f is a scalar nonlinear function of a multi-dimensional vector \mathbf{y} defined within the domain D . The domain D is a hypercube defined by the upper and lower bounds on the components of the vector \mathbf{y} :

$$y_i \in [b_i^l, b_i^u]. \quad (2)$$

The vector $\mathbf{C}(\mathbf{y})$ is formed by all nonlinear constraint functions of the vector \mathbf{y} . If problem (1) is twice continuously differentiable and presents a single solution, i.e. only one vector \mathbf{y} in the domain D minimises f and satisfies \mathbf{C} , a nonlinear programming method like sequential quadratic programming (SQP) can be efficiently used. This means implicitly that the problem must be formulated properly and cannot contain non-differentiable quantities. However, even in this case the problem may present more than one solution within the required search space D .

If the problem is either non-differentiable, i.e. no gradient method can be applied, or more than a solution is expected, a global optimisation method must be considered. The idea is to perform an extensive search of the solution space D looking for possible solutions to problem (1). In this respect the interest could be more in finding a number of good initial guesses for the nonlinear programming solver, rather than finding the global optimum with a high level of accuracy.

Among all global methods two categories are here considered: heuristic methods and systematic methods.

Heuristic methods contain all methods that cannot be proven to find a global optimum with a predictable amount of work. Most stochastic methods are in this class. For this particular class, it is sometimes possible to prove convergence with probability arbitrarily close to 1 but with a number arbitrarily large of function evaluations.

Systematic methods contain all methods that (in exact arithmetic) are guaranteed to find the global optimum with a predictable (deterministic) amount of work. The bound on the amount of work is anyway quite high: exponential in the problem characteristics. The simplest systematic method for bound-constrained problems is grid search (or enumerative search) where all points on increasingly finer grids are tested and the best point on each grid is used as a starting point for local optimisation. The number of grid points grows exponentially with the dimensions of the problem and so does the amount of work. Even though systematic methods are generally more reliable than heuristic ones they need some level of insight into the problem and the structure of the objective function, to be efficient (an exception can be made for methods based on interval analysis [14]). If the problem is represented by a black box then they may not find the

43

45

47

49

51

53

55

57

59

61

63

65

67

69

71

73

75

77

79

81

83

85

87

89

1 global optimum in a reasonable amount of time. This
 2 is understandable if we look at the density theorem
 3 [15], which states that any method based only on local
 4 information, that converges for every continuous f
 5 to a global minimiser of f in a feasible domain D must
 6 produce a sequence of points y^1, y^2, y^3, \dots that is
 7 dense in D . A well known stochastic method is represented
 8 by genetic algorithms (GA) [8] that make use
 9 of analogies to biological evolution by allowing mutations
 10 and crossing over among candidates for good
 11 local optima in the hope to derive even better ones.
 12 The original concept of genetic algorithms is to encode
 13 a potential solution (individual) of the problem
 14 under study, in the form of a binary string in which
 15 each binary number represents a chromosome of the
 16 “DNA” (or genotype) of the solution (or phenotype).
 17 More sophisticated genetic algorithms make use of the
 18 data structure of the problem to encode the individual
 19 in the more appropriate way [6]. An improvement in
 20 standard genetics, used to increase exploration capabilities,
 21 is represented by niching-GA [7]. The basic
 22 concept is that in nature different species can exploit
 23 different niches in the environment. This translates in
 24 the formation of subpopulations with each subpopulation
 25 specialised at a subtask of the problem or exploring
 26 a subregion. Subpopulations can compete as
 27 in pure GA or cooperate. In general all methods that
 28 resort to some heuristic ideas derived from biological
 29 evolution can be defined as evolution strategies.

30 Among systematic methods there are some that split
 31 the solution domain on the basis of some local information.
 32 Each time the domain is split, a number
 33 of new branches are created, each branch corresponding
 34 to a further exploration of the solution space and
 35 each subdomain representing a node that can be expanded
 36 and explored further. If the diameter of all the nodes
 37 converges to zero, convergence of the algorithm is
 38 straightforward.

39 The proposed optimisation approach is composed
 40 of a stochastic and a systematic step. The stochastic
 41 step is performed using an evolution strategy and is
 42 meant to obtain information on the possible presence
 43 of optima in a subdomain $D_l \subseteq D$. The systematic step
 44 is performed through a branching approach and is used
 45 to partition the domain D into subdomains D_l , where
 46 the presence of an optimum is expected. Each subdomain
 47 may or may not contain the global optimum but the
 systematic exploration of the subdomains, al-

48 lows finding a number of optima and eventually the
 49 global one. This particular hybridisation can be seen
 50 as a form of *forced* niching since populations evolving
 51 in subregions form different species.

52 This particular hybridisation is the first difference
 53 with respect to usual global techniques. Other peculiarities
 54 of this approach rely on the way each individual
 55 explores the solution space throughout an environment
 56 perception mechanism that will be presented in
 57 the next section. For a comparison with known methods
 58 the interested reader can refer to [16]. 59

3. Evolutionary-branching approach

3.1. Evolution step 61

62 Each solution \mathbf{y} is represented by a string, of length
 63 n , containing in the first m components integer values
 64 and in the remaining s components real values. This
 65 particular encoding allows the treatment of problems
 66 with a mixed integer-real data structure. A hypercube
 67 \mathbf{S} is associated to each individual \mathbf{y} , the hypercube,
 68 enclosing a region of the solution space surrounding
 69 the individual, is defined by a set of intervals
 70 $\mathbf{S} = S_1 \times S_2 \dots \times S_n \subseteq D_l$, where S_i contains the
 71 value of the component y_i . The solution space is then
 72 explored locally by acquiring information about the
 73 landscape within each region \mathbf{S} and globally using a
 74 population of individuals \mathbf{y} with their associated intervals.
 75 Each individual can communicate its findings to the
 76 others in order to evolve the entire population towards
 77 a better status.

78 Evolution is governed by four fundamental operators:
 79 mutation, migration, mating and filtering. The
 80 mutation operator generates a new individual randomly
 81 perturbing an old one. The mating procedure takes
 82 two individuals and generates one or two children
 83 mixing the genotypes of the two parents. Four
 84 schemes are used to mate individuals:

85 Single point crossover exchanges part of the genes
 86 between the two parents;

- 87 • Arithmetic crossover generates a new individual
 88 with an interpolation of the two parents.
- 89 • Extrapolation generates a new individual on the
 90 side of the best individual between the two parents
 91 \mathbf{y}^1 and \mathbf{y}^2 at a distance from the best parents

proportional to the vector connecting the two parents:

$$\mathbf{y}^3 = \alpha(\mathbf{y}^2 - \mathbf{y}^1) + \mathbf{y}^2. \quad (3)$$

- Second order extrapolation mating generates a child using two parents and the child generated with an extrapolation mating. If \mathbf{p} is the vector difference between \mathbf{y}^1 and \mathbf{y}^3 and f^1, f^2, f^3 are the fitness values for the three individuals $\mathbf{y}^1, \mathbf{y}^2, \mathbf{y}^3$ respectively, then a second order one-dimensional model of the fitness function is built and the new child is generated taking the minimum of the resulting parabola (see Fig. 1):

$$\mathbf{y}^4 = \mathbf{y}^1 + \mathbf{p}\chi_{\min}, \quad (4)$$

$$f_{\min} = a(\mathbf{y}^1, \mathbf{y}^2, \mathbf{y}^3)\chi_{\min}^2 + b(\mathbf{y}^1, \mathbf{y}^2, \mathbf{y}^3)\chi_{\min} + f(\mathbf{y}^1). \quad (5)$$

The mating operator is also used to prevent crowding of more than one principal individual in the basin of attraction of the same solution: if two or more principal individuals are colliding (intersecting their migration regions) and their reciprocal distance falls down below a given threshold, a repelling mechanism is activated which mates the worse individual (between the two colliding) with the boundaries of the subdomain D_i : each component of the selected individual is blended with the value of the furthest bound, projecting the individual into a random point within D_i , according to the following relation:

$$y_i^2 = \alpha b_i + (1 - \alpha)y_i^1. \quad (6)$$

3.1.1. Environment perception and migrations

Each region \mathbf{S} is evaluated using two alternative mechanisms: breeding or *perception* and learning. Breeding generates a subpopulation and selects the best child, if better than the parent. A new region \mathbf{S} is then associated to the child generating a migration of the entire subpopulation towards a place where better resources are expected. For this reason each hypercube \mathbf{S} is here called *migration region*. The subpopulation is generated with the following procedure: a first child is generated, within \mathbf{S} , mutating the parent, then an extrapolation mating is performed. The two resulting children and the parent are then used to

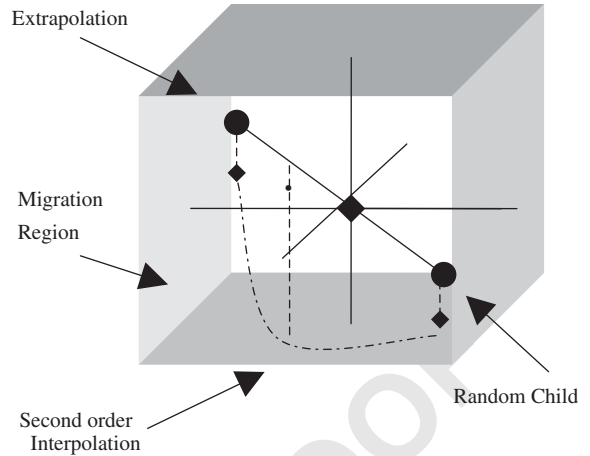


Fig. 1. Perception mechanism.

generate a third child using second order extrapolation mating. The procedure is repeated until a number of children equal to the number of coordinates have been generated (see Fig. 1). This procedure can be seen as a way for the individual \mathbf{y} to *perceive* or sense locally the environment to obtain clues about where to proceed with the exploration of the solution space.

Learning is performed using two mechanisms: interval analysis and gradient methods. In the first case the inferior value of f within the migration region is associated to the individual \mathbf{y} and perception is then not necessary. In the second case, if the function f is locally continuous and differentiable a number of SQP steps are taken if perception gives no results and the migration region shrinks down to a small value.

The contraction or expansion of each region \mathbf{S} is regulated through a migration radius ρ and depends either learning or on the perception mechanism. The migration radius is defined as the ratio between the value of the distance from the boundary \mathbf{b}^j of the migration region of the j th individual and the value of the distance from the corresponding boundary \mathbf{b} of the domain D :

$$\rho^j = \frac{b_i^j - y_i^j}{b_i - y_i^j}. \quad (7)$$

If none of the children of the subpopulation are better than the parent the radius is reduced according to

$$\rho^j = \begin{cases} \max([1e - 8, \delta y_{\min}]) & \text{if } \delta y_{\min} \geq \varepsilon \rho^j, \\ \varepsilon \rho^j & \text{if } \delta y_{\min} < \varepsilon \rho^j, \end{cases} \quad (8)$$

1 where ε has been set to 0.5 and δy_{\min} is the distance
2 of the best child \mathbf{y}^* , among the ones in the migration
3 region, from the parent j , normalised with respect to
4 the dimensions of the migration region:

$$5 \delta y_{\min} = \sqrt{\sum_{i=1}^n \left(\frac{y_i^* - y_i^j}{S_i^j} \right)^2}, \quad (9)$$

6 where for individual j and for dimension i , S_i^j is the
7 difference between the value of the upper bound and of
8 the lower bound and the summation is over non-zero
9 dimensions. Now, if from generation k to generation
10 $k+1$ the differential improvement Δf^j (the difference
11 between the function f^j at generation k minus f^j at
12 generation $k+1$) increases, then the migration radius
13 is recomputed according to the prediction:

$$14 \rho_{k+1}^j = \rho_k^j \eta \log(e - 1 + j), \quad (10)$$

15 where η is equal to 2 in this implementation. For inte-
16 ger numbers migration operates in the same way but
17 the migration regions and migration radius are gener-
18 ated and treated differently. In particular if $\rho_{i \min}$ is 1
19 and ρ is defined as

$$20 \rho_{k+2}^j = \min[\text{int}(\log(2 + j)\Delta f^j), \rho_{i \min}]. \quad (11)$$

21 The migration region is therefore contracted differ-
22 ently for real and for integer variables allowing a bet-
23 ter spatial exploration.

3.1.2. Filtering

24 Instead of traditional selection mechanisms based
25 on fitness here a permanent population of n individu-
26 als is maintained from one generation to another. Each
27 individual has a chance to survive provided that it re-
28 mains inside the filter. The filter ranks all the individu-
29 als on the basis of their fitness from best to worst. All
30 the individuals with a fitness worse than a given thresh-
31 old are either hibernated (i.e. no operator is applied) or
32 mutated while migration is applied to all individuals
33 within the filter. The probability of being mutated or
34 hibernated depends on their ranking. This allows each
35 of the individuals within the filter to evolve towards a
36 different local optimum. Mating is operated between
37 all the individuals who present an improvement after
mutation or migration and all the remaining ones.

3.2. Branching step

38 Even though the filter increases the chances of find-
39 ing several optima and eventually the global one, con-
40 vergence is not guaranteed due to the stochastic nature
41 of the process. Therefore, a systematic step is taken on
42 the basis of the output of the evolutionary algorithm.
43 The initial domain $D_0 \equiv D$ is partitioned generating
44 a number of subdomains D_l . Each subdomain is then
45 qualified and explored further according to its qualifica-
46 tion.

47 The partitioning, or branching, process begins by
48 taking the worst individual, which is out of the filter,
49 and cutting D_0 into L subdomains, corresponding to L
50 potentially new branches (or nodes). Each one of the
51 L nodes may or may not contain an individual coming
52 from the previous step of evolution and the volume of
53 the node depends on the position of the cutting point
54 (a safeguard mechanism prevents cuts too close to a
55 boundary moving the cutting point to the middle of
56 the interval). For each node D_l the ratio between the
57 relative number of individuals and the relative volume
58 is computed and the resulting quantity defines how
59 necessary a further exploration of the node is
60

$$61 \varpi_{D_l} = \frac{\sum_{D_l} j}{\sum_D j} / \sqrt[n]{\frac{V_{D_l}}{V_D}}, \quad l = 1, \dots, L, \quad (12)$$

62 where the volumes V_{D_l} and V_D are computed taking
63 only edges with a non-zero dimension. This quantity
64 is then added to a fitness φ_{D_l} defined as
65

$$66 \varphi_{D_l} = \begin{cases} \frac{\frac{1}{J} \sum_{j=1}^J f_j - f_{\text{best}}}{f_{\text{worst}} - f_{\text{best}}} & \text{if } J \neq 0, \\ 1 & \text{otherwise,} \end{cases} \quad (13)$$

67 where J is the number of individuals in domain D_l . If
68 interval analysis is available each subregion is evalu-
69 ated taking the inferior and superior values, the quan-
70 tity φ_{D_l} is then defined as

$$71 \varphi_{D_l} = \inf_{D_l} (f). \quad (14)$$

72 The node is then qualified by the quantity:

$$73 \psi_{D_l} = \sigma \varpi_{D_l} + (1 - \sigma) \varphi_{D_l}, \quad (15)$$

74 where σ is the weighting factor that weights how reli-
75 able the result coming from the evolution step is con-
sidered. If σ is 0, only the nodes with low fitness are

1 explored because the evolutionary algorithm is con- 43
 2 sidered reliable enough to explore exhaustively the 44
 3 domain D without leaving any region unexplored. On 45
 4 the other hand, if σ is 1 the result from the evolution-
 5 ary algorithm is considered to be not reliable due to a
 6 premature convergence or to a poor exploration of the
 7 solution space. Now every time a node D_l is subdiv-
 8 9 divided into other Q subnodes only the most promising
 10 pair is taken into account. If ψ_{D_l} is used to select the
 11 most promising ones among all L subdomains, the best
 12 pair out of the Q subnodes generated for each subdo-
 13 mains is selected using the following slightly different
 quantity:

$$\tilde{\psi}_{D_q} = \sigma \frac{\sum_{D_q} j}{\sum_{D_l} j} \Big/ \gamma_q + (1 - \sigma) \varphi_{D_q},$$

$$q = 1, \dots, Q, \quad (16)$$

15 where γ_q is, for each of the subnodes q , the ratio be-
 16 tween the length of the edge along which the sub-
 17 domain D_l is cut and the corresponding edge of D_q .
 18 Once a D_q is selected the other subnode of the pair
 19 will be the complement $D_{q+1} = D_l - D_q$. For a fast
 20 search only nodes presenting a high fitness and large
 21 volume are explored further.

22 In order to avoid the rediscovery of minima already
 23 found, the original domain is partitioned using more
 24 than one individual. If the worst individual is useful
 25 to determine an upper bound on the objective func-
 26 tion, converged individuals suggest where a further
 27 exploration is unnecessary. Therefore, in the general
 28 scheme, all converged individuals are ranked depend-
 29 ing on the value of their fitness function. The principal
 30 cut is then, as stated above, performed using coordi-
 31 nates of the worst individual, the second cut takes the
 32 worst converged individual and so on up to the best
 33 converged individual.

3.3. Constraint satisfaction

35 The algorithm described solves bound-constrained
 36 problems but since in most of the cases constraints
 37 are nonlinear an extension of the algorithm has been
 38 developed that takes into account nonlinear inequality
 39 constraints.

40 At each evolution step the population of solutions
 41 is divided into two subpopulations and a different ob-
 jective function is assigned to each one, namely one

subpopulation aims at minimising the original objec-
 tive function while the other aims at minimising the
 residual on the constraints defined as

$$\min_{y \in D} f(\mathbf{y}) = \sum_{j=1}^q e^{R_j}, \quad (17)$$

47 where q is the number of violated constraints and R_j
 48 is the residual of the j th violated constraints. The two
 49 subpopulations are evolved in parallel and individuals
 50 are allowed to jump from one population to the other,
 51 i.e. if a feasible individual becomes infeasible it is in-
 52 scribed in the subpopulation of infeasible individuals
 53 and assigned to the solution of problem (17), on the
 54 other hand if an infeasible individual becomes feasi-
 55 ble it is inserted in the population of feasible individ-
 56 uals and allocated to the minimisation of the original
 57 bound-constrained objective function f . As a result, the
 58 final optimal solution is either feasible or minimises
 59 infeasibilities.

60 This procedure does not maintain feasibility for any
 61 individual, therefore once a feasible set has been found
 62 the perception mechanism is used to ensure that every
 63 move maintains the feasible population inside the feasi-
 64 ble set. If f^* is the value of the objective function
 65 of an individual \mathbf{y} inside the feasible set, the objective
 66 function of a new individual generated from \mathbf{y} is then
 67 augmented in the following way:

$$\min_{y \in D} f = \begin{cases} f^* & \text{if every } R_j \leq 0, \\ f^* + \max R & \text{if any } R_j > 0. \end{cases} \quad (18)$$

69 The described strategy co-evolving two populations
 70 with two different goals, allows a flexible search for
 71 feasible optimal solutions: in fact through the de-
 72 scribed use of the perception mechanism feasibility
 73 can be enforced on all feasible solutions or just on
 74 the best among the feasible ones. In the former case
 75 the exploration of the solution space may be over pe-
 76 nalisised reducing the convergence rate or leading to a
 77 local minimum, on the other hand the latter strategy,
 78 while preserving the feasibility of at least the best
 79 solution, allows a more extensive search along the
 boundary of the feasible region.

3.4. Interval analysis and stopping criterions

81 There are two combined stopping criteria: one for
 82 local convergence and one for global convergence. 83

1 Both are based on some heuristics and not on any rigorous proof of global converge. Local convergence of
 3 each subpopulation is determined by the improvement of each individual and by the migration radius. In a
 5 convex problem, both should tend to zero in the neighbourhood of the solution. Since each individual is sup-
 7 posed either to converge to a different minimum or not to converge (letting just the individual with highest
 9 rank in the filter to converge) a global stopping criterion for the evolution step is the convergence of the
 11 filter. The convergence of the filter is determined by the convergence of all the individuals if they are not
 13 clustered, i.e. if their migration regions are not intersecting, and, otherwise, by the convergence of the best
 15 individual. Convergence for an individual is reached when its migration radius drops below a given thresh-
 17 old. It must be noticed that when evolution step is used in conjunction with branching the convergence of the
 19 filter is not usually necessary since the branching takes care of the global exploration of the solution space.
 21 The global convergence of the branching is reached either if all the nodes reduce below a given tolerance
 23 or if evolution steps have converged in all subdomains and no improvement is reported after branching, i.e.
 25 no new local minima are discovered. Interval analysis, when used, guarantees that the node containing the
 27 global minimum is always in the list of explored nodes therefore if the difference between the inferior value
 29 of the best node and the best individual contained in that node is below a given tolerance, convergence to
 31 the global optimum is achieved.

33 The process is initialised defining the boundaries of the search space D , setting the value for σ , the number
 35 of individuals and the dimension of the filter, then the algorithm proceeds in the exploration until one of the
 37 stopping criteria is met or the maximum number of function evaluations is reached.

39 Human intervention is therefore limited to the initial definition of the search space and of the number of
 41 exploring individuals but it must be underlined that the branching step allows a loose definition of the bound-
 43 aries as opposed to common evolutionary approaches [8]. On the other hand the stochastic nature of the
 45 evolution step makes the method robust against landscapes which might deceive systematic methods [10].

47 The total computational cost of each run depends on the total number of function evaluations and the
 level of exhaustiveness can be tuned changing σ and

the number of levels of branching thus increasing or 49
 reducing the total number of function evaluations as 51
 desired. Since, here the interest is a characterisation of 53
 the solution space more than a quick convergence to 55
 the global optimum, σ has been set to 0.9, the maxi- 57
 mum number of branching steps has been set to 4, gen-
 erating a maximum of 81 subdomains and the number
 of function evaluation for the evolution step has been
 limited to 6000.

4. Characterisation of Earth–Mars roundtrips

59 The global search algorithm presented in the previ-
 ous chapters is now applied to the problem of charac-
 61 terising Earth–Mars transfers.

63 The first analysis looks for roundtrips from Earth
 to Mars with minimal total Δv . Roundtrip trajectories
 are made of an Earth–Mars transfer, departing from
 65 either a circular or an elliptical orbit around the Earth
 and aiming at either a circular or an elliptical orbit
 67 around Mars, a certain stay time around Mars and a
 return transfer to either a circular or an elliptical orbit
 69 around the Earth. Depending on the launch date and
 on the transfer time, for each leg, different families of
 71 roundtrips can be envisaged. In order to include even
 free return trajectories, instead of a braking and a de-
 73 parture manoeuvre, a swing-by of Mars is performed
 every time the stay time drops below 1 day.

4.1. Problem modelling

75 Each transfer is computed in a three-dimensional
 heliocentric ecliptic reference frame, as the solution of
 77 a Lambert’s problem for the restricted 2-body problem
 [17]. Each planet is considered as a point mass with
 79 no gravity. Ephemeris of the planets are computed
 analytically as polynomial expansions of the orbital
 81 parameters as a function of the modified Julian date
 (MJD2000). 83

The resulting global optimisation problem can be
 85 formulated as

$$\min_D f = \Delta v_1 + \Delta v_2 + \Delta v_3 + \Delta v_4, \quad (19)$$

87 where Δv_2 and Δv_3 represent, respectively, the brak-
 ing manoeuvre and the departure manoeuvre at Mars,
 89 while Δv_1 and Δv_4 are, respectively, the departure
 manoeuvre and the braking manoeuvre at Earth.

1 Each Δv is computed as the difference between the
 2 velocity at the pericentre of the arrival or departure
 3 planetocentric hyperbola and the velocity at the peri-
 4 centre of a planetocentric orbit with pericentre and
 5 apocentre radius (r_p^E, r_a^E) for Earth and (r_p^M, r_a^M) for
 6 Mars, respectively. The v_∞ of each hyperbola is de-
 7 rived from the solution of the above mentioned Lam-
 8 bert's problem and from the velocity of each planet on
 9 its orbit.

10 Thus the Δv s are functions of the departure date
 11 t_0 , the time of flight for the outbound leg T_1 and for
 12 the inbound leg T_2 , the stay time t_s . Each solution is
 13 therefore defined by the following vector:

$$\mathbf{y} = [t_0, T_1, T_2, t_s, r_p^E, r_a^E, r_p^M, r_a^M]^T. \quad (20)$$

14 And the solution space D contains all possible values
 15 of \mathbf{y} . In case of swing-by of Mars a linked-conic ap-
 16 proximation of the gravity manoeuvre is used and the
 17 objective function becomes:

$$18 \quad f = \Delta v_1 + 10C_1^2 + 20C_2^2 + \Delta v_4, \quad (21)$$

19 where the two constraint violations for the swing-by
 20 manoeuvre, C_1 and C_2 are defined as

$$21 \quad C_1 = v_i^2 - v_o^2; \quad C_2 = \langle \mathbf{v}_i, \mathbf{v}_o \rangle + \cos(2\beta)v_iv_o, \quad (22)$$

22 where \mathbf{v}_i and \mathbf{v}_o are the incoming and outgoing ve-
 23 locity vectors relative to Mars and β is the deviation
 24 angle, function of the modulus of the incoming velo-
 25 city, of the radius r_p^M of the pericentre at Mars and of
 26 the gravity constant μ_M of Mars.

$$27 \quad \beta = a \cos\left(\frac{\mu_M}{v_i^2 r_p^M + \mu_M}\right). \quad (23)$$

28 A further analysis of return trajectories via Venus has
 29 been done, introducing an additional swing-by in the
 30 model and extending the solution vector (and therefore
 31 the domain D) as follows:

$$32 \quad \mathbf{y} = [t_0, T_1, T_2, t_s, r_p^E, r_a^E, r_p^M, r_a^M, \omega, r_p^V, T_3, T_4]^T, \quad (24)$$

33 where now T_2 is the time of flight from Mars to Venus,
 34 r_p^V is the pericentre radius at Venus, ω is the rotation
 35 angle of the plane of the hyperbola around the in-
 36 coming vector with respect to the ecliptic plane [16],
 37 T_3 is the time of flight after the swing-by, to a deep
 38 space manoeuvre and T_4 is the time of flight from the

Table 1
Domain D for the roundtrip problem

Variable	Lower bound	Upper bound
t_0 (MJD)	5479	15775
T_1 (day)	50	700
T_2 (day)	50	700
t_s (day)	0	600
r_p^E (km)	6778	6778
r_a^E (km)	6778	6778
r_p^M (km)	3789	5.7e5
r_a^M (km)	3789	5.7e5

deep space manoeuvre to the Earth. The new objective
 function must include the deep space manoeuvre and
 therefore becomes:

$$\min_D f = \Delta v_1 + \Delta v_2 + \Delta v_3 + \Delta v_4 + \Delta v_5. \quad (25)$$

4.1.1. Short and long stay options

At first problem (19) was solved looking for
 roundtrips with a variable stay time ranging from 0
 to 600 days and evaluating the total Δv necessary
 for each launch opportunity. Then, the search was
 focused on short stay opportunities including returns
 via Venus (commonly called opposition class mis-
 sions). The solution space D for problems (19) and
 (21) is defined in Table 1 and comprises all the pos-
 sibilities including free return trajectories. Launch
 windows from 2015 to 2043 were explored and all
 the solutions with a total Δv less than 13 km/s have
 been collected and plotted in Figs. 2 and 3, where
 diamonds represent short stay and free return options.

Then if the upper limit on total Δv is extended to
 15 km/s several short stay trajectories with a return via
 Venus become feasible. The result has been plotted in
 Fig. 4. It should be noticed that a return via Venus is
 not always available and for each solution via Venus
 it is often possible to find a direct return with a com-
 parable level of Δv . This is true apart from two launch
 windows in which only a return via Venus allows, for
 a short stay, a total Δv less than 15 km/s. Furthermore,
 for two particular launch opportunities (13 years away
 from one another) an almost continuous range of short
 stay periods are allowed.

The latter one of the two comprises almost all the
 returns via Venus since for this date Venus is in a
 particularly favourable position.

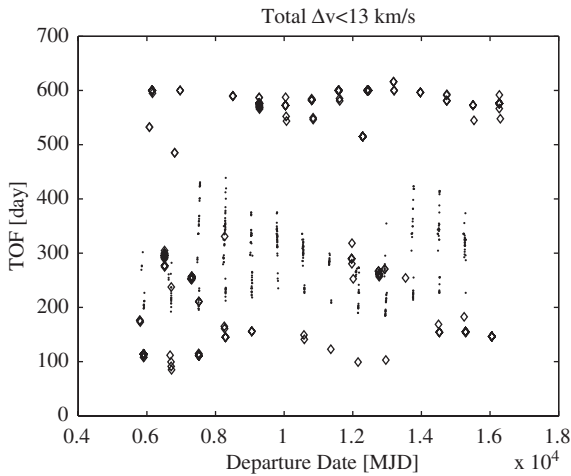


Fig. 2. Departure date vs. TOF.

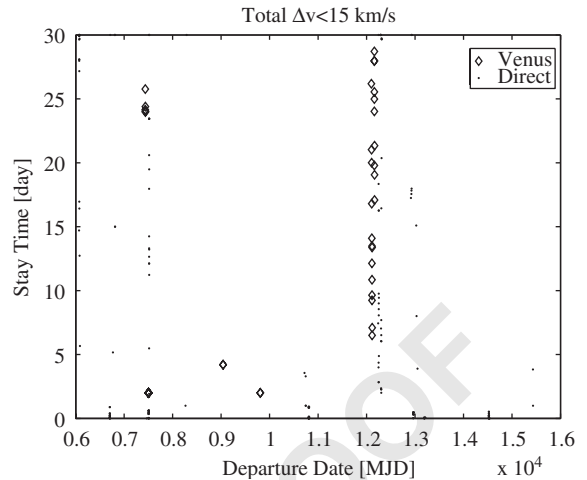


Fig. 4. Return via Venus vs. direct return.

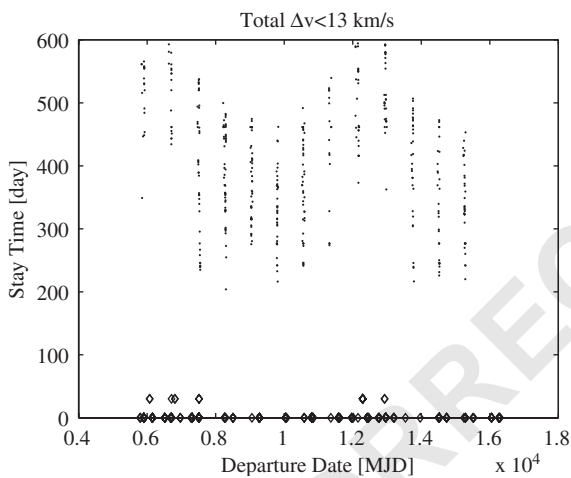


Fig. 3. Departure vs. stay time.

trajectory choices are the most influential parameters, the total dose due to galactic cosmic radiation (GCR) were calculated for all presented options in Table 3. The values are equivalent BFO dose values in sievert (Sv). Interplanetary dose values behind 10 g/cm^2 Al are assumed at 0.24 Sv/a . Mars surface levels behind 5 g/cm^2 Al are assumed 0.15 Sv/a . Dose levels for equivalent PE shielding materials are given in brackets.

Due to the stochastic nature of the method, for this case the evolutionary-branching algorithm was run twice to check the exploration of the solution space was sufficiently exhaustive. In both cases the algorithm, implemented in a Matlab code, took about one hour on a 2 GHz Pentium 4 m with 256 Mb of RAM.

4.1.2. Free return trajectories and cyclers

As can be noticed in Fig. 3, for each launch window it is possible to find a solution with a stay period below 1 day, which in fact corresponds to a trajectory that departs from Earth, flies by Mars and comes back to Earth ballistically, i.e. without manoeuvres. These trajectories, known as free return trajectories, can be grouped in three main categories (see Fig. 5).

The first one comprises all transfers with a low departure velocity from Earth, a correspondent short transfer arc to Mars and a long arc leading the spacecraft back to Earth again with a low arrival velocity (see Fig. 6). The overall period in space is about two

1 Very short stays (less than 10 days) are also possible both via Venus and via direct return. This class of trajectories can become interesting as abort options in case an immediate return is necessary and a manoeuvre at Mars can still be executed. The most interesting options for a short stay either via Venus are summarised in Table 2 for the period from 2028 to 2037 while optimal solutions for each launch date, in the same period, are summarised in Table 3.

11 Since total absorbed radiation dose is one of the key issues for human Mars mission design and since the

Table 2

Best short stay options via Venus from 2028 to 2037

Launch Date	E–M (day)	M–E (day)	t_s (day)	Δv_1 (km/s)	Δv_2 (km/s)	Δv_3 (km/s)	Δv_4 (km/s)	Δv_5 (km/s)
21/10/2028	252	251	2	4.16	3.63	4.80	5.98	0.193
04/07/2029	529	404	2	4.28	5.28	3.27	4.72	1.579
30/06/2031	460	490	2	4.12	4.56	3.28	6.53	0.644
16/04/2033	199	352	28	3.59	2.43	4.21	3.94	6.15e-4
17/02/2035	236	318	2	4.97	3.02	4.29	3.78	3.13e-4
02/09/2037	225	475	30	4.06	2.03	3.33	4.36	1.369

Table 3

Optimal solutions for direct Earth–Mars roundtrip from 2028 to 2037

Launch Date	E–M (day)	M–E (day)	t_s (day)	Δv_1 (km/s)	Δv_2 (km/s)	Δv_3 (km/s)	Δv_4 (km/s)	GCR (Sv)	m_f/m_0
23/11/2028	300.1	353.5	344.1	3.589	2.244	2.077	3.9348	0.57(0.43)	0.035
09/08/2029	596.6	320.9	600	4.366	5.067	2.1498	4.123	0.85(0.63)	0.01
24/12/2030	283.1	217.7	497.8	3.663	2.53	1.992	3.749	0.53(0.38)	0.035
17/02/2031	210.7	217.7	514.9	3.806	2.776	1.992	3.749	0.49(0.35)	0.031
16/04/2033	199.7	198.0	553.0	3.587	2.435	2.239	3.589	0.49(0.34)	0.036
26/11/2034	248.1	251.0	30	6.1361	3.9151	3.498	5.1868	0.34(0.28)	0.003
27/06/2035	201.9	267.5	535.6	3.6447	2.07	2.5836	3.689	0.53(0.37)	0.034
02/06/2036	700	284.9	444.0	4.7548	8.347	2.313	3.5439	0.83(0.64)	0.001
15/08/2037	347.5	282.9	358.1	3.9298	2.131	2.313	3.5439	0.56(0.42)	0.035

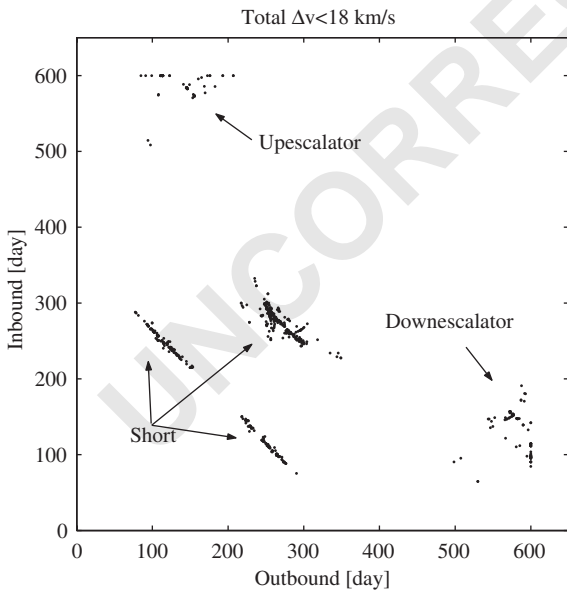


Fig. 5. Free return trajectories.

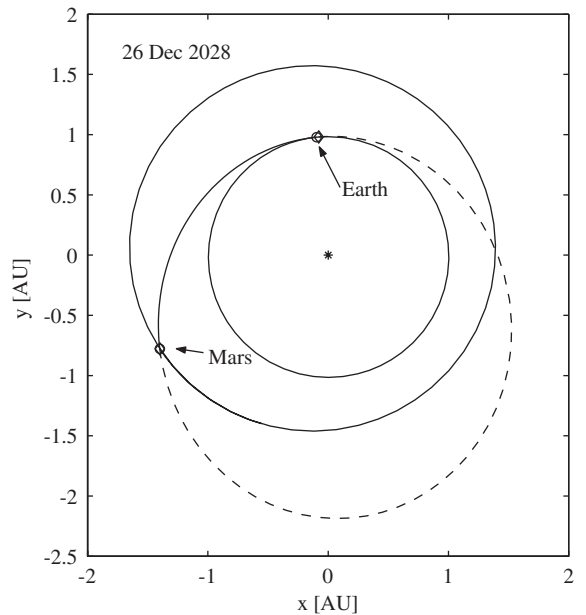


Fig. 6. Up escalator.

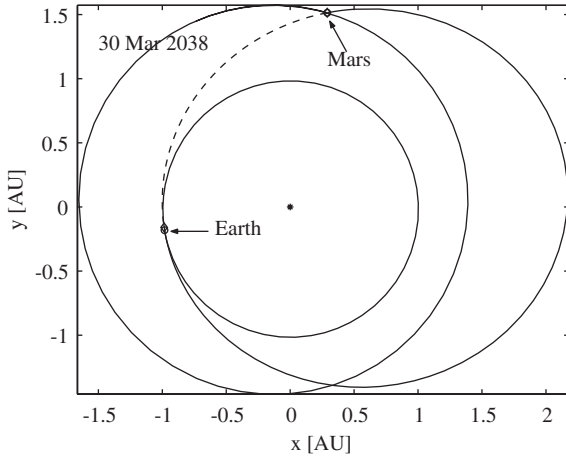


Fig. 7. Down escalator.

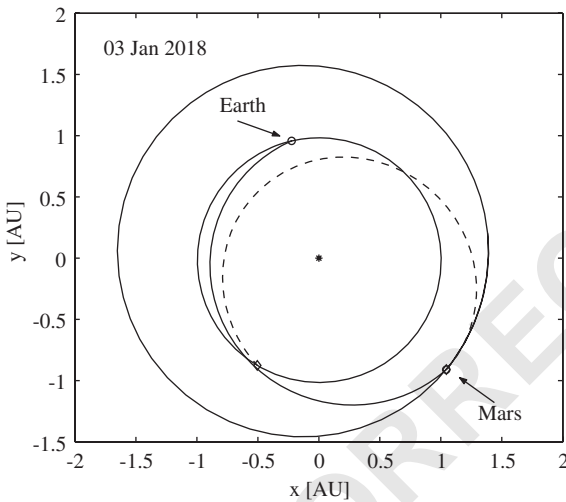


Fig. 8. Short roundtrip.

1 terrestrial years, therefore, in analogy with Earth–Mars
 2 one-synodic-period cyclers, these free return trajectories
 3 are here called up escalators. The second category
 4 comprises all free return trajectories with an initial
 5 long transfer to Mars and a short return leg to Earth,
 6 the total time in space is again about 2 years and there-
 7 fore these trajectories are here called down escalators
 8 (see Fig. 7). The third category of free return trajec-
 9 tories presents a relatively short transfer time on both
 legs either to go or to come back (see Fig. 8).

As can be seen in Fig. 5 short free return trajectories
 can be subdivided further in three groups depending
 on the length of each leg. All best free return oppor-
 tunities for the period from 2028 to 2037 have been
 summarised in Table 4 where transfer time, infinite
 velocity at Mars and Δv at Earth are reported. As can
 be read, although up and down escalators are appeal-
 ing for their relatively low Δv at departure they can
 become prohibitive if the spacecraft has to be inserted
 in orbit around Mars with a propulsive manoeuvre,
 due to the high infinite velocity.

On the other hand, some short free return options,
 although more demanding in terms of Δv at departure
 have in general a lower velocity at Mars and could
 be interesting either as nominal trajectories in order
 to increase safety for manned missions or as abort
 options.

In fact if a failure, not affecting the propulsion sys-
 tem, forces the mission to be aborted on the way to
 Mars, in some cases, a deep space manoeuvre, ex-
 ploiting the whole remaining propellant, could be used
 to inject the spacecraft on a short free return transfer
 back to Earth.

Similar results, although for different launch dates
 and obtained with a fully systematic search method,
 can be found in [18,19].

4.2. Optimal staging

Even in case cryogenic propellants are consid-
 ered for propulsion (with an $I_{sp} = 450$ s) the mass
 budget for a roundtrip to Mars could be prohibitive
 even for minimum Δv transfers (see last column of
 Table 3). A solution could be to resort to staging
 in order to improve the payload returned to Earth.
 Therefore, the natural extension of problem (19) is to
 introduce staging sequences in the model and to opti-
 mize for the final mass m_f instead of the total Δv .
 The staging model assumed here is fairly simple and
 does not take into account gravity losses. Furthermore,
 a constant specific impulse and a constant structural
 factor of 0.15 has been considered for each stage.

$$m_{i+1} = m_i e^{-\Delta v / g_0 I_{sp}}, \quad (26)$$

$$m_{i+1} = m_{pl} + m_{p_{i+1}} + m_{s_{i+1}} + m_{s_i}, \quad (27)$$

$$m_s = 0.15 m_p \quad (28)$$

Table 4

Best free return options found from 2028 to 2037

Launch date	E–M (day)	M–E (day)	Δv_1 (km/s)	Δv_4 (km/s)	v_∞ (km/s)	r_p (km)
26/12/2028	141.1	588.4	4.281	4.283	10.77	43389
01/08/2029	582.49	147.4	4.349	4.347	6.961	43301
18/09/2030	272.5	253.82	5.827	8.11	5.253	3789.0
09/02/2031	122.87	600	4.285	4.319	11.653	43389
21/11/2032	252.67	255.98	4.977	6.38	5.1056	3790.7
12/04/2033	99.05	600	4.446	4.876	11.44	13732
02/01/2034	600	90.48	5.103	4.499	10.488	9840.1
25/02/2036	600	113.5	4.504	4.311	11.776	36714
24/01/2037	254.32	262.8	7.2679	5.2115	5.252	3789.0

Table 5

Mass fractions at arrival at Earth with 2 stages

Date	r_a^E (km)	ε_1^E	r_a^M (km)	ε_1^M	m_f/m_0
23/11/2028	5.4e4	0.162	1.9e5	0.03	0.168
24/12/2030	4.3e4	0.195	1.0e5	0.06	0.167
16/04/2033	4.1e4	0.197	4.1e5	0.015	0.168
09/07/2035	4.8e4	0.178	5.0e5	0.01	0.166

1 the objective function then becomes:

$$\max_{\mathbf{y} \in D} f = -m_f/m_0, \quad (29)$$

3 where m_0 is the initial mass and each solution is defined by the vector:

$$\mathbf{y} = [t_0, T_1, T_2, t_s, r_p^E, r_a^E, r_p^M, r_a^M, \varepsilon_1^E, \varepsilon_1^M]^T, \quad (30)$$

7 where ε_1^E and ε_1^M represent for Earth departure and for Mars insertion respectively the ratio between the apocentre of the departure (arrival) orbit r_a^E (r_a^M) and the apocentre radius of the intermediate orbits. The pericentre altitude of the departure (arrival) is constrained to be at 400 km and the initial and final orbits are assumed to be circular with the same altitude. Therefore, if a 2-stage strategy is used for Earth escape the first stage injects the spacecraft from the 400×400 km circular orbit into an intermediate orbit with apocentre $\varepsilon_1^E r_a^E$ and the second stage injects the spacecraft into a departure orbit with apocentre r_a^E . Furthermore, the number of stages is fixed and equal for each escape or capture manoeuvre. In Table 5 some optimal solutions for the interval [2028, 2037] are reported for a 2-stage strategy.

5. Low-thrust transfers

All the analysis of the previous chapter assumed the use a high thrust engines, however, low-thrust propulsion systems may become interesting both for manned and unmanned missions. Therefore, an analysis of direct low-thrust Earth–Mars transfer will follow. A low-thrust trajectory is here modelled using an inverse method: the Cartesian coordinates of the spacecraft are described by means of a set of *pseudo-equinoctial elements* α . The set of elements used to parameterise the Cartesian coordinates are here called *pseudo-equinoctial* because they do not satisfy exactly the Gauss' planetary equations unless the thrust is zero. Each element is then developed in form of a parameterised function of the anomaly L . This function is the shape of the pseudo-element.

Once position is defined in terms of the pseudo-elements velocity and accelerations can be computed by differentiation:

$$\mathbf{v} = \frac{d\mathbf{r}}{dt} = \frac{d\mathbf{r}}{dL} \frac{dL}{dt}; \quad \mathbf{a} = \frac{d\mathbf{v}}{dt} = \frac{d\mathbf{v}}{dL} \frac{dL}{dt}, \quad (41)$$

$$\frac{d\mathbf{r}}{dL} = \sum_{i=1}^5 \frac{\partial \mathbf{r}}{\partial \alpha_i} \frac{\partial \alpha_i}{\partial L} + \frac{\partial \mathbf{r}}{\partial L}. \quad (31)$$

In order to obtain the set of pseudo-elements that satisfies exactly the conditions at boundaries, the following nonlinear programming problem must be solved:

$$\begin{aligned} \mathbf{r}(\alpha(L_0), L_0) &= \mathbf{r}_0; & \mathbf{v}(\alpha(L_0), L_0) &= \mathbf{v}_0; \\ \mathbf{r}(\alpha(L_f), L_f) &= \mathbf{r}_f; & \mathbf{v}(\alpha(L_f), L_f) &= \mathbf{v}_f; \end{aligned} \quad (32) \quad 47$$

1 where for low values of the acceleration it is sufficient
to solve the easier linear problem:

$$3 \quad \boldsymbol{\alpha}(L_0) = \boldsymbol{\alpha}_0; \quad \boldsymbol{\alpha}(L_f) = \boldsymbol{\alpha}_f. \quad (33)$$

5 For each set of pseudo-elements a different trajectory
can be generated, connecting two points in the state
7 space. The controls necessary to achieve the imposed
shape of the trajectory can then be obtained by solving
the following system:

$$9 \quad \mathbf{a}_c = \mathbf{a} - \frac{\mu}{r^3} \mathbf{r}; \quad m_f = m_0 e^{\int_{t_0}^{t_f} -c|a_c| dt} \quad (34)$$

with the additional constraint

$$11 \quad t_f - t_0 = \int_{L_0}^{L_f} \frac{dt}{dL} dL. \quad (35)$$

13 This approach is extremely fast and the computational
cost extremely low since no propagation or collocation
is necessary.

15 Of course the thrust profile, though constrainable,
is a direct consequence of the shape and must be con-
sidered only as a first guess useful for further, more
17 refined optimisation. However, the attempt here is to
widely explore the solution space rather than to find
19 an accurate solution. For this reason the design of the
low-thrust trajectory has not been written either in the
optimal control form (with adjoint equations) or in any
21 direct transcription form (collocation or shooting).

23 It is anyway expected that as the shape of the
pseudo-elements approaches the solution of the corre-
sponding optimal control problem the inverse method
25 will yield the associated optimal control for the thrust.
For the analysis conducted in this paper the following
27 shape has been used:

$$31 \quad \boldsymbol{\alpha}(L) = \boldsymbol{\alpha}_0 + \boldsymbol{\alpha}_f(L - L_0) + \mathbf{p} \sin(L - L_0), \quad (36)$$

where $\mathbf{p} = [p_1, p_2, p_3, p_4, p_5]^T$ is a set of parameters
shaping each pseudo-element.

33 The optimality of the solution found can be seen
from the comparison with the optimal solution com-
puted for Mars Exobiology. In the optimised solution
35 the trajectory is characterised by two coast arcs and
three thrust arcs and a maximum thrust dependent on
the distance from the Sun. On the other hand, the first
37 estimate obtained with the inverse approach does not
contain any model for power and thrust and no coast
39 arcs are introduced a priori.

Table 6

Domain D for the low-thrust problem

Variable	Lower bound	Upper bound
N	0	2
t_0 (MJD)	2500	3000
T_1 (day)	500	1e3
θ	$-\pi$	$-\pi$
ϕ	$-\pi$	$-\pi$
p_1	-0.1	0.1
p_2	-0.1	0.1
p_3	-0.1	0.1
p_4	-0.1	0.1
p_5	-0.1	0.1

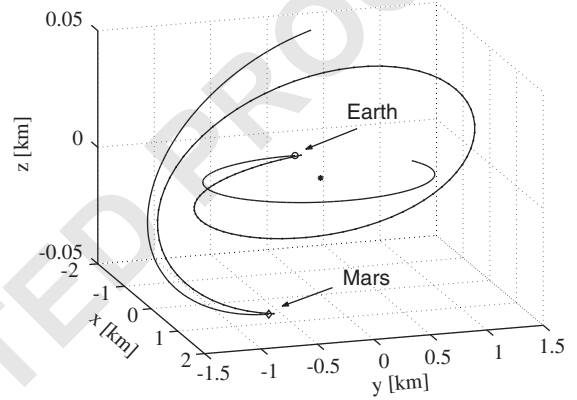


Fig. 9. Mars Exobiology test case.

The optimisation problem then becomes

$$\min_D -m_f,$$

$$t_f - t_0 = 0; \quad a_c \leq a_{\max}, \quad (37) \quad 43$$

and the solution vector is

$$\mathbf{y} = [n, t_0, T_1, \theta, \phi, p_1, p_2, p_3, p_4, p_5]^T, \quad (38) \quad 45$$

where n is an integer number representing the num-
ber of revolutions, t_0 is the departure date and T_1 the
47 transfer time. The domain D is specified in Table 6.

49 The resulting trajectory is represented in Fig. 9 with
the associated thrust profile plot in Fig. 10. The main
characteristics of the two trajectories are summarised
51 and compared in Table 7 where FG stands for first
guess and represents the solution computed with the
53 inverse approach.

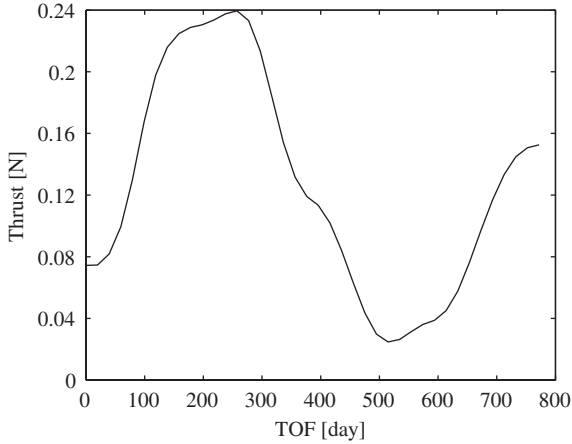


Fig. 10. Thrust profile.

Table 7
Comparison with Mars Exobiology

Sol.	Departure	TOF(day)	m_f/m_0	v_∞ (m/s)
Opt.	18/03/2007	873	0.16	622
FG	09/03/2007	772.1	0.162	622

The algorithm successfully identified a solution with a low mass consumption comparable with the optimised solution for Mars Exobiology. The transfer time however is quite different due to the selected shape of the orbit. The solution found is expected to have an error in the velocity due to the not exact solution of problem (32). However, this error has been verified to lead, in general, to an equivalent error in propellant consumption which is below 15%. Therefore this solution can be considered acceptable as a first estimate of a possible transfer with low-thrust propulsion, since the error is within the usual margin taken in preliminary mission design.

5.1. Low-thrust transfers with ballistic capture at Mars

The propellant consumption to reach Mars with a low excess velocity, provided by low thrust transfers opens the interesting possibility to exploit lagrangian points of the Mars–Sun system to attempt a low-energy capture in Martian orbit. Maintaining the previous model for low-thrust arcs now the dynamics at arrival

Table 8

Low-thrust transfers with ballistic capture

Departure	$a_{\max} \cdot (\text{m/s}^2)$	TOF(day)	m_f/m_0	v_∞ (km/s)
15/08/2030	2.3e-4	721	0.165	0.2

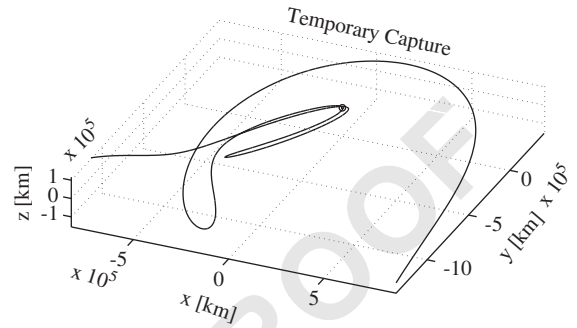


Fig. 11. Temporary capture.

is modelled taking into account 3rd body effects. Final conditions at Mars are taken perturbing the state vector at L_1 and propagating backward for a time Δt the following dynamic equations:

$$\frac{d\tilde{\mathbf{x}}}{dt} = \tilde{\mathbf{F}}(\tilde{\mathbf{x}}, t) = \begin{cases} \tilde{\mathbf{v}} \\ -\frac{\mu_M}{r^3} \tilde{\mathbf{r}} - \mu_S \left(\frac{\mathbf{d}}{d^3} + \frac{\mathbf{r}_S}{r_S^3} \right), \end{cases} \quad (39)$$

where μ_S is the gravity constant of the Sun, r_S is the position vector of the Sun with respect to Mars and $[\tilde{\mathbf{r}}, \tilde{\mathbf{v}}]$ is the state vector of the spacecraft with respect to Mars.

The solution vector has been extended as follows:

$$\mathbf{y} = [n, t_0, T_1, \Delta t, \delta v_1, \delta v_2, \delta v_3, p_1, p_2, p_3, p_4, p_5]^T, \quad (40)$$

where now $\delta v_1, \delta v_2$ and δv_3 are the three components of the velocity vector at the lagrangian point L_1 defined in the local radial, transversal, normal martian reference frame. The value of first component belongs to the interval $[-0.12, 0.0]$ km/s while the values of the others belong to the interval $[-0.12, 0.12]$ km/s.

The resulting point in deep space at the end of the backward propagation, represents the target of the electric propulsion arc. An example of low-thrust transfer of this kind is reported in reported in Table 8. The arrival at Mars has been plotted in Figs. 11 and 12 for an unpowered and for a powered capture. In the

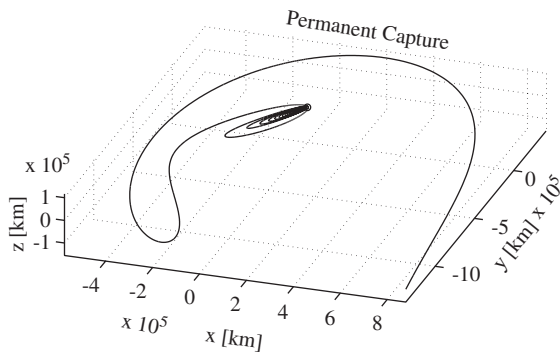


Fig. 12. Permanent capture with low-thrust manoeuvre at periapses.

1 first case no manoeuvres are performed at periapsis and the resulting capture by Mars is only temporary and lasts less than 500 days. In the second case a low-thrust manoeuvre is inserted when the distance from Mars falls down below $1e5$ km, the resulting capture is now permanent.

7 In this case the evolutionary-branching algorithm was not applied to characterise the solution space. A first interval was computed running evolutionary-branching with the model described in the previous chapter (i.e. without 3rd body effects) then just the evolution step was run, including 3rd body effects in the model and imposing a minimum of 50 days for Δt .

15 This first result is encouraging and suggests further investigations in this direction.

6. Conclusions

17 In this paper a combined systematic-heuristic approach is proposed to solve trajectory design problems in which more than one solution is expected and where not just the global optimum should be obtained. The proposed combination of evolutionary algorithms and branching is suitable for problems characterised by differentiable and non-differentiable functions combining integer and real variables, and demonstrated to be an interesting tool for preliminary mission analysis especially when the objective function is a black-box. In fact, in this respect an ad hoc systematic approach specifically dedicated to solve a certain problem is expected to be more efficient.

31 The capabilities of this approach have been demonstrated by solving the complex problem of identifying

all optimal solutions for a Mars roundtrip in a given time frame. This first analysis has revealed that free return trajectories are always available for each launch window and can be classified in three major groups depending on the length of each transfer leg. Although all of them present the significant drawback of having high velocity either at Earth or at Mars they could represent an option for high specific impulse engines or as abort options. Among nominal transfers in the time frame 2028, 2037 the 2033 launch window seems to offer interesting features since the transfer time for both legs is relatively low with an associated low total Δv and a low cost return via Venus is possible for a short stay. For nominal transfers the analysis of optimal staging sequences has shown how the optimal orbit for departure from Earth is elliptical but with the apocentre almost at the altitude of a geostationary orbit while for Mars the apocentre is much closer to the sphere of influence. Finally, the last analysis presented has opened the interesting possibility to use low-thrust transfers for low-energy planetary capture at Mars. However, this problem and the inverse approach used to design low-thrust arcs, are the subjects of an ongoing more detailed analysis and therefore, the results presented in this paper must be considered preliminary.

The proposed optimisation algorithm appears to be promising for generally complex space trajectory design problems. Despite the effective exploration capabilities demonstrated in the cases presented in this paper, the efficiency of the method has still large margins for improvement and the convergence to the global optimum is still not guaranteed if not in a probabilistic sense or after an infinite number of subdivisions of the branching step. In this respect the proposed use of interval analysis, when actually viable, represents a promising way of guaranteeing and controlling convergence.

An improved version of the algorithm is already under development and will be presented in future works.

Acknowledgements

The authors are grateful to Guy Janin of ESOC/ESA for Mars Exobiology trajectory with electric propulsion.

33
35
37
39
41
43
45
47
49
51
53
55
57
59
61
63
65
67
69
71
73

References

- [1] P.J. Gage, R.D. Braun, I.M. Kroo, Interplanetary trajectory optimisation using a genetic algorithm, *Journal of the Astronautical Sciences* 43 (1) (1995) 59–75. 3
- [2] G. Rauwolf, V. Coverstone-Carroll, Near-optimal low-thrust orbit transfers generated by a genetic algorithm, *Journal of Spacecraft and Rockets* 33 (6) (1996) 859–862. 5
- [3] V. Coverstone-Carroll, J.W. Hartmann, W.J. Mason, Optimal multi-objective low-thrust spacecraft trajectories, *Computer Methods in Applied Mechanics and Engineering* 186 (2000) 387–402. 7
- [4] M. Vasile, G. Comoretto, A.E. Finzi, A combination of evolution programming and SQP for WSB transfer optimisation, *AIRO2000*, Milano, Italy, September 18–21, 2000. 9
- [5] P. Gurfil, N.J. Kasdin, Niching genetic algorithms-based characterization of geocentric orbits in the 3D elliptic restricted three-body problem, *Computer Methods in Applied Mechanics and Engineering* 191 (49–50) (2002) 5673–5696. 11
- [6] Z. Michalewicz, *Genetic Algorithms + Data Structures = Evolution Programs*, third ed., Springer, Telos, 1996. 13
- [7] J. Horn, The nature of niching: genetic algorithms and the evolution of optimal, cooperative populations, Ph.D. Thesis, University of Illinois at Urbana-Champaign, 1997. 15
- [8] C.R. Houck, J. Joines, M. Kay, A genetic algorithm for function optimization: a Matlab implementation, *ACM Transactions on Mathematical Software*, 1996. 17
- [9] C. Blied, P. Spellucci, L.N. Vicente, A. Neumaier, L. Granvilliers, E. Huens, P. Van Hentenryck, D. Sam-Haroud, 19
- B. Faltings, COCONUT deliverable D1. Algorithms for solving nonlinear constrained and optimisation problems: the state of the art, The Coconut Project, June 8, 2001. 33
- [10] D.R. Johns, C.D. Perttunen, B.E. Stuckman, Lipschitzian optimization without the lipschitz constant, *Journal of Optimization Theory and Applications* 79 (1993) 157–181. 35
- [11] J.D. Pintér, *Global Optimization in Action*, Kluwer, Dordrecht, 1996. 37
- [12] C.S. Adjiman, S. Dallwing, C.A. Floudas, A. Neumaier, A global optimization method, alphaBB, for general twice-differentiable constrained NLPs-I. Theoretical advances, *Computers and Chemical Engineering* 22 (1998) 1137–1158. 39
- [13] B. Gardini, F. Ongaro, ESA Aurora exploration programme, 53rd IAC Houston 10–19 October 2002, IAC-02-IAA.13.1.02. 41
- [14] E. Hansen, *Global Optimization Using Interval Analysis*, Marcel Dekker Inc., New York, 1992. 43
- [15] A. Törn, A. Zilinskas, *Global Optimization*, Lecture Notes in Computer Science, Vol. 350, Springer, Heidelberg, 1989, 255pp. 45
- [16] M. Vasile, A global approach to optimal space trajectory design, AAS-03-141, 13th AAS/AIAA Space Flight Mechanics Meeting, Puerto Rico, 9–13 February 2003. 47
- [17] R.H. Battin, *An Introduction to the Mathematics and Methods of Astrodynamics*, AIAA Education Series, Vol. XXXII, AIAA Inc., New York, 1987, . 49
- [18] M.R. Patel, J.M. Longuski, J.A. Sims, Mars free return trajectories, *Journal of Spacecraft and Rockets* 35 (3) (1998). 51
- [19] M. Okustu, J.M. Longuski, Mars free return via gravity assist from Venus, *Journal of Spacecraft and Rockets* 39 (1) (2002). 53

UNCORRECTED